NaLa(SO4)2,H2O thermal conversion and Na3La(SO4)3 crystal growth

H Azeroual, L Vendier, A Geneste, D Granier, L Alvarez, P Hermet, O Cambon

Journal Pre-proof

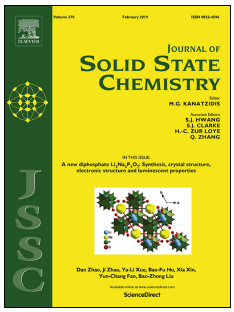

$NaLa(SO_4)_2,H_2O$ thermal conversion and $Na_3La(SO_4)_3$ crystal growth

H. Azeroual, L. Vendier, A. Geneste, D. Granier, L. Alvarez, P. Hermet, O. Cambon

PII: S0022-4596(22)00695-8

DOI: https://doi.org/10.1016/j.jssc.2022.123570

Reference: YJSSC 123570

To appear in: *Journal of Solid State Chemistry*

Received Date: 1 July 2022

Revised Date: 1 September 2022

Accepted Date: 5 September 2022

Please cite this article as: H. Azeroual, L. Vendier, A. Geneste, D. Granier, L. Alvarez, P. Hermet, O. Cambon, $NaLa(SO_4)_2,H_2O$ thermal conversion and $Na_3La(SO_4)_3$ crystal growth, *Journal of Solid State Chemistry* (2022), doi: https://doi.org/10.1016/j.jssc.2022.123570.

Credit Author Statement

Name of authors	Credit
Hanae AZEROUAL	Experiments and results interpretation
Laure VENDIER	Crystallographer
Amine GENESTE	Thermal analyses
Dominique GRANIER	Crystallographer
Laurent ALVAREZ	Raman spectroscopy
Patrick HERMET	Raman spectroscopy and calculation
Olivier CAMBON	Supervisor and writer

$NaLa(SO_4)_2,H_2O$ thermal conversion and $Na_3La(SO_4)_3$ crystal growth.

H. Azeroual[a], L. Vendier[b], A. Geneste[a], D. Granier[a], L. Alvarez[c], P. Hermet[a], O. Cambon[a†]

[a] Univ Montpellier, ICGM, CNRS, ENSCM, Montpellier, France

[b] Univ Toulouse, CNRS, LCC, Toulouse, France

[c] Université de Montpellier, L2C, Montpellier, France

[†] Corresponding author. Email: Olivier.cambon@umontpellier.fr

Abstract:

$NaLa(SO_4)_2,H_2O$ crystalline powder was obtained under hydrothermal conditions at 220°C. A coupled TGA/DTA experiment of $NaLa(SO_4)_2,H_2O$ exhibits a weight loss at 260°C corresponding to the dehydration and an endothermal peak at 774°C. To elucidate the transformation mechanism as a function of temperature, single crystals have been grown at 80°C, 300 and 800°C. For each phase, single crystals have been isolated and structure determination was performed. As already published, $NaLa(SO_4)_2,H_2O$ crystallizes in a $P3_121$ space group. However, the dehydration at 260°C is not a simple loss of the water molecule but a radical change in the structure. The removal of the water molecules inside the tunnels formed by the framework leads to a change in the coordination of the LaO_9 Lanthanum-based polyhedrons. The compound obtained after dehydration is a new triple sulphate of the formula $Na_3La(SO_4)_3$ crystallizing in the *R*-3 space group (a= 14.0976(1) Å; c= 8.1267(1) Å) with LaO_{12} icosahedrons. Millimeter size single crystals of this new phase have been grown under hydrothermal conditions (300°C, 157bars). After the endothermal peak at 774°C, $Na_3La(SO_4)_3$ decomposes by forming the anhydrous double sulfate $NaLa(SO_4)_2$ crystallizing in the *P*-1 space group with LaO_{10} polyhedrons. The structure of the three (NaLa)-compounds at RT, 300°C and 800°C is compatible with the expected Raman signatures. Finally, a complete transformation of $NaLa(SO_4)_2,H_2O$ up to 800°C is proposed. After 1000°C, the compound decomposes chemically with a large weight loss.

Keywords: Sodium Lanthanum sulfate, thermal decomposition, single crystal x-ray diffraction, Lanthanum-based polyhedron, H-bonds, Raman spectroscopy.

I. Introduction:

Due to their electronic configuration, Rare Earth (RE) elements group is very important for designing new materials with numerous properties such as catalytic [1, 2], non-linear optical (NLO) [3-6] or fluorescence [4, 7-10] properties. Among all the RE-oxides, the lanthanide double sulfates with general formula $ML_n(SO_4)_2, H_2O$ were particularly studied by varying the chemical composition [2, 11-19]. Moreover, in a circular economy scheme, Porvali et al [20] demonstrated that the RE coming from NiMH batteries could be recovered by precipitation

with the formation of their alkali double sulfate due to their low solubility. The structure of Na*Ln*$(SO_4)_2$,H_2O (*Ln*= La[15, 2], Ce [21, 13], Nd [2], Gd [2] and Pr [22]) compounds have been solved by single-crystal x-ray diffraction and belongs to the $P3_121$ or $P3_221$ space group. In this structure, the lanthanide is nine-fold coordinated [*Ln*O_9] like distorted tricapped trigonal prisms joined among them by the SO_4 tetrahedrons with eight oxygen-atoms and by the oxygen atom of the H_2O molecule. K. Kazmierczak and H. A. Höppe [23] changed the alkaline cation by replacing Na by K in the formula. For all lanthanides except for La, K*Ln*$(SO_4)_2$,H_2O crystallize in the $P2_1/c$ space group while KLa$(SO_4)_2$,H_2O adopts the $P3_221$ space group. Along this series, *Ln* atoms are nine or eight-fold coordinated. Kolcu et al. [24] already studied the thermal decomposition of Na*Ln*$(SO_4)_2$,H_2O-type compounds up to 1600°C by thermal analyses, IR spectroscopy and X-ray diffraction. A decomposition mechanism was proposed leading to lanthanide oxide Ln_2O_3 as the final product through the subsequent formation of NaLnOSO_4, $Ln_2O(SO_4)_2$ and $Ln_2O_2SO_4$ as intermediate compounds. Nevertheless, in this paper only the structure of the starting monohydrate is well determined. Crystallographic data for the intermediate compounds are not given. Recently, Y.G. Denisenko and al [25] published a study on the sodium samarium double sulfate monohydrate trigonal $P3_121$ NaSm$(SO_4)_2$,H_2O and its thermal decomposition. According to the DSC and TG data the dehydration produces in the range 500-650K. From the authors, the dehydration product is anhydrous triclinic *P*-1 NaSm$(SO_4)_2$ which is stable up to 1110K and above this temperature the anhydrous compound decomposes successively into Na_2SO_4 and $Sm_2(SO_4)_3$ then the sulfates melt (1150-1175K). Finally, $Sm_2(SO_4)_3$ decomposes into $Sm_2O_2SO_4$ at 1300K and Sm_2O_3 at 1460K. Nevertheless, on the DSC curve, authors did not notice the presence of a large endothermic peak at about 1000K which is the sign of a chemical reaction. From our point of view, the dehydration procedure of NaSm$(SO_4)_2$,H_2O is not well established, and the phase obtained after water removal is not the triclinic phase. C. Buyer and al. [26] present also a study about NaY$(SO_4)_2$, H_2O and its anhydrate NaY$(SO_4)_2$. In this paper, only TG data are available and then there is no information about transformation without weight loss which could be observed with DTA analysis. So, the dehydration mechanism is also not well established. This paper present a study on the trigonal $P3_121$ NaLa$(SO_4)_2$,H_2O phase and focus on its thermal decomposition mechanism by determining the crystal structure evolution in terms of temperature up to 1273K. After dehydration, a new *R*-3 phase has been discovered. Single crystals of this *R*-3 phase have been also grown under HT/HP hydrothermal conditions (above the dehydration temperature).

II. Methods.

II.1. Synthesis and crystal growth.

NaLa$(SO_4)_2$,H_2O compound was crystallized under hydrothermal conditions. All chemicals were purchased from Aldrich and used without further purification. 4g La$(NO_3)_3$,$6H_2O$ (0.009 mole) were dissolved in 20 mL of sulfuric acid (4M). Then 0.36g NaOH (0.009 mole) was added into the solution and stirred for 30 min. The pH was observed to be 2. The entire mixture was poured into a 30 mL Teflon lined autoclave. The autoclave was kept heated with a steel jacket at 220°C for 5 days. The product was then filtered and washed with distilled water. It is a white powder manufactured with a yield of around 73%.

In the aim to define a crystallization process in solution, hydrochloric acid 4M has been chosen as the solvent. The solubility of NaLa$(SO_4)_2$.H_2O was analyzed for various temperature ranges from 25°C to 80 °C. The previous synthesized solute NaLa$(SO_4)_2$,H_2O was dissolved in 4M HCl in an airtight container by using magnetic stirrer maintained at constant temperature. The solubility curve for different temperatures was shown in Figure 1. The solubility curve shows

a direct solubility in the 25 – 80°C temperature range which allows to envisage a growth process of $NaLa(SO_4)_2,H_2O$ single crystals by slow cooling method. The next step was to grow $NaLa(SO_4)_2.H_2O$ single crystals from $NaLa(SO_4)_2.H_2O$ powder previously dissolved in 4M HCl by cooling the solution from 80°C to 25°C with a 2°C step per day in a glass tubular oven; the process takes approximately 27 days. In the end, crystals of size 100x200x250 µm were obtained.

A second phase at 300°C was crystallized by using two different methods: the first method consists of a thermal treatment of the previous $NaLa(SO_4)_2,H_2O$ crystalline powder at 300°C under air in an oven for 3 days. The product contains some plate-like single crystals. The second method is by using a high temperature and pressure autoclave where the same mixture used to synthesize $NaLa(SO_4)_2.H_2O$ is heated until 300°C with a pressure of 157 bars; these conditions were kept during 10 days. The final product was filtered and washed with water; some hexagonal single crystals were isolated.

A third phase at 800°C was obtained by a heat treatment of $NaLa(SO_4)_2,H_2O$ powder under air in an oven at 800°C for 3 days. Single crystals have been then isolated.

II.2. Thermal analysis.

TGA and DTA analyses were carried out on crushed $NaLa(SO_4)_2,H_2O$ single crystals by using a NETZSCH STA 449F1 analyzer under an Ar flow in the temperature range from 20 to 1000°C with a heating rate of 2°C/min.

II.3. X-Ray diffraction.

Powder diffraction
The powder XRD patterns were recorded in the 2θ range 10° to 80° with a step size of 0.03° using X-ray diffraction Philips X'PERT PANalytical diffractometer equipped with a spinner configuration (θ–θ) using CuK_α radiation (λ= 1.54184Å).

Single crystal diffraction
The crystal determinations have been performed with different diffractometers. The crystal data have been merged into a unique table for the three compounds (Table 1). The structures were solved by direct methods using SHELXS 2013/1 software and refined by full-matrix least-squares using SHELXL 2014/7software.
For the starting phase $NaLa(SO_4)_2$, H_2O, suitable single crystal was mounted on a cryoloop and X-ray crystal structures was determined using a Bruker 3-circle D8 Venture diffractometer with a PHOTON II area detector, using Mo K_α radiation (λ = 0.71073 Å) from 1µS microsource with focusing mirrors operating at 50 kV and 1 mA.
For the phase obtained at 300°C, a single crystal was mounted on a Rigaku XtaLAB Synergy diffractometer equipped with a micro-focus sealed tube X-ray source (Cu Kα radiation, λ= 1.54184 Å).
For the phase crystallized at 800°C, a Bruker Kappa Apex 2 diffractometer equipped with a tube X-ray source (Mo Kα radiation, λ= 0.71073 Å) was used.

II.4. Raman spectroscopy.

Raman experiments have been performed at room temperature on a T64000 spectrometer from Horiba-Jobin-Yvon using a triple monochromator configuration. The spectra were recorded in a backscattering geometry and by using the 491 nm line from a COBOLT laser diode. The beam was focused using a 50x lens. The spectral resolution was about 2 cm^{-1}. A Linkam TS1500 stage was used for in situ measurements between 30 and 200°C. The sample is placed inside

the ceramic sample cup and is heated from underneath as well as from the sides. A controller enables the stage to heat samples at the accurate temperature.

III. Results and Discussion.

III.1. Thermal analyses

On the thermal analysis graph (Figure 2), the weight loss producing between 220 and 260°C is due to the dehydration of $NaLa(SO_4)_2,H_2O$. The weight loss is 4.95% that corresponds to the complete removal of the water molecule from the initial compound. Then the weight evolution is flat as a function of temperature up to 820°C from which the chemical decomposition is starting with a weight loss of 20%. On the DTA curve, the first large peak at 309°C corresponds to the endothermal reaction of the dehydration. Thermal measurements do not give result at equilibrium. Kinetics must be considered. So, the DTA peak which corresponds to the weight loss (up to 260°C) is shifted to 309°C. Then, another endothermal peak at 774°C is observed. Because this peak does not correspond to any weight loss, it could be due to a phase transition or a chemical reaction without any product releasing. This peak was not previously reported in the literature. Finally, after 900°C, intense endothermal peaks accompanied with a weight loss are due to the chemical decomposition of the lanthanide sulfate. The DTA cooling curve shows three exothermal peaks. This paper reports what could be happened during the dehydration (220-260°C) and during the transformation at 774°C. For this purpose, the compounds obtained by thermal treatment of initial $NaLa(SO_4)_2,H_2O$ crystals at 300°C (after dehydration) and 800°C (after 774°C) have been more accurately studied by x-ray diffraction and Raman spectroscopy.

III.2. X-ray diffraction

Table 1 groups the data collection and refinement conditions as well as the crystal data used for the single crystal X-ray diffraction of the three types of compounds.

i. Initial $NaLa(SO_4)_2,H_2O$. (Tables S1 to S3)

The starting compound $NaLa(SO_4)_2,H_2O$ was synthesized as described above. Single crystal x-ray diffraction data are in good agreement with the structure already published by Backburn [15] and Perles et al. [2]. The positions of H atoms are not well defined: two refinements have been performed with and without H atoms. Similar $R[I>2\sigma(I)]$ factor value of 0.0146 has been obtained but when H atoms are imposed in the structure their positions are not well fixed and the O-H bond length is not satisfying. So, the structure without H atoms is the only one presented here. In consequence, a strong anisotropy of the electronic density is observed for the O8-water atom for which the values of the ADP parameters reach a maximum value of 0.128Å^2 for the U^{33} component. As supposed by Perles et al. [2], the O-atom of the water molecule occupies a top of the distorted LaO_9 polyhedron and is positioned in the center of the tunnels formed by the framework (Figure 3). The existence of H-bonds is supported by Raman scattering with the softening of the O-H stretching vibration (3250 – 3700 cm-^{1}) as the temperature decreases (Figure 4). The position above 3200 cm^{-1} indicates that the H-bonds can be classified as weak in this compound. The analyze of the atomic distances values in the structure allows to assign the O7 atoms with which H-bonds are formed. Indeed, the O8-O7 distance is 2.974(2) Å (Figure 4).

ii. Dehydration of $NaLa(SO_4)_2,H_2O$ (T= 300°C)

During dehydration (220-260°C) of $NaLa(SO_4)_2$, H_2O, the structure of the compound is largely modified due to the removing of the structural water molecule. Micrometer size single crystals of the new phase were obtained by a thermal treatment at 300°C of the $NaLa(SO_4)_2$,H_2O microcrystalline powder previously synthesized. Moreover, bigger crystals (1mm size) of the same new phase have also been directly grown under hydrothermal conditions at 300°C and 157bars (Figure 5). The new structure has been determined by single x-ray diffraction.

Structure of $Na_3La(SO_4)_3$

The structure was well refined ($R[I>2\sigma(I)]$= 1.6%) in a *R*-3 space group (*a*= 14.0976(1) Å; *c*= 8.1267(1) Å). This structure corresponds to a new kind of lanthanide sulfate with the general formula $Na_3Ln(SO_4)_3$ which has never been identified. The structure of this new phase of $Na_3La(SO_4)_3$ was deposited under the 2168542 ICSD number. Reduced atomic coordinates and ADP parameters are given in Tables S4 and S5, respectively. This structure consists of two complexes LaO_{12} and NaO_6 cations and one SO_4 sulfate anion (Figure 6). NaO_6 is a distorted octahedral complex involving the symmetry-related O1, O2, O3 and O4 oxygen atoms with Na-O distances varying from 2.329(2) to 2.71(2) Å and with O-Na-O angles varying from 72.80(7) and 171.10(7)° (Table S6). The LaO_{12} polyhedron is a near perfect icosahedron built from the interlocking of two perfect octahedra. Therefore, the $La1O_{12}$ icosahedron is based on the two $La1(O1)_6$ and $La1(O4)_6$ perfect octahedra while the $La2O_{12}$ icosahedron is based on the two $La2(O1)_6$ and $La2(O2)_6$ perfect octahedra (Table S6). The angles vary from 52.53(5) to 180.0° in the first $La1O_{12}$ icosahedron and from 52.87(5) to 180.0° in the second $La2O_{12}$ icosahedron. Sulfate anion forms a slightly irregular tetrahedron with S-O distances ranging from 1.455(2) to 1.514(2)Å; the angles varying form 104.9(1) to 112.8(1)°. During the dehydration of the Lanthanum sodium disulfate monohydrate the framework is completely transformed. The tunnels along the c-axis disappear and the LaO_9 polyhedra transform into LaO_{12} icosahedra. The density increases from 2.5 $g.cm^{-3}$ for $NaLa(SO_4)_2$, H_2O to 3.5 $g.cm^{-3}$ for $Na_3La(SO_4)_3$. In consequence, a dehydration mechanism implying the formation of two solid phases is proposed as following:

$$3\ NaLa(SO_4)_2,H_2O\ (s) \rightarrow Na_3La(SO_4)_3\ (s) + La_2(SO_4)_3\ (s) + 3H_2O\ (g)$$

This reaction is also confirmed by x-ray powder diffraction (Figure 7) with the presence of the patterns of $Na_3La(SO_4)_3$ and lanthanum sulfate $La_2(SO_4)_3$.

iii. Thermal treatment of $NaLa(SO_4)_2,H_2O$ (T= 800°C).

At 774°C, an endothermal peak is observed on the DTA curve. This peak has never been described in the literature even if it was already measured at about 1000K (747°C) for $NaSm(SO_4)_2,H_2O$ [25] for example. So single crystals have been synthesized by a heat treatment of initial compound $NaLa(SO_4)_2,H_2O$ at 800°C during 3 days. A single crystal x-ray diffraction was carried out and the refinement led to the structure of $NaLa(SO_4)_2$ with the triclinic space group *P*-1 ($R[I>2\sigma(I)]$= 1.9%) . The refined structure of $NaLa(SO_4)_2$ is in good agreement with that already published [27]. The structure includes LaO_{10}, NaO_8 and SO_4 polyhedra (Figure 8). All structural parameters are given in Tables S7 to S9. Note that the sulfate anions are of two structural types based on S1 and S2 atoms.

So, the DTA peak observed at 774°C without any weight loss is not a phase transition but corresponds to the following chemical transformation without any product releasing:

$$Na_3La(SO_4)_3\ (s) + La_2(SO_4)_3\ (s) \rightarrow NaLa(SO_4)_2\ (s) + Na_2SO_4\ (s) + La_2(SO_4)_3\ (s)$$

From the initial sulfate monohydrate, the complete reaction becomes:

$$3\ NaLa(SO_4)_2,H_2O\ (s) \rightarrow\ NaLa(SO_4)_2\ (s) + Na_2SO_4\ (s) + La_2(SO_4)_3\ (s) + 3H_2O(g)$$

The x-ray powder diffraction pattern (Figure 9) confirms the formation of the three products $NaLa(SO_4)_2$, La_2SO_4 and Na_2SO_4.

iv. Final treatment at 1000°C.

After DTA-TGA analysis up to 1000°C, three phases have been identified by x-ray powder diffraction (Figure 10): $La_2O_2SO_4$ (*C*2/c, ref: 01-085-1535), Na_2SO_4 (*C*mcm, ref : 01-083-1570) and a remaining quantity of $NaLa(SO_4)_2$ *P*-1 which has not been transformed. Moreover, three exothermal peaks are observed on the DTA cooling curve. These peaks correspond to the crystallization of the three previous crystalline phases identified by x-ray powder diffraction.
This result is in good accordance with the literature. Indeed, as refered by Kolcü [24], $NaLa(SO_4)_2$ transformed at 1000°C as followed: $2NaLa(SO_4)_2 \rightarrow 2NaLaOSO_4 + 2SO_2 + O_2$. In fact, $NaLaOSO_4$ is not referenced in the PDF-database. Nevertheless, $2NaLaOSO_4$ can be expressed like $La_2O_2SO_4 + Na_2SO_4$.
For $La_2(SO_4)_3$, the transformation at 1000°C is proposed by Poston and al. [28] by forming $La_2O_2SO_4 + 2SO_2 + O_2$.
So, the transformation at 1000°C is given by the following reaction
$NaLa(SO_4)_2\ (s) + Na_2SO_4\ (s) + La_2(SO_4)_3\ (s) \rightarrow La_2O_2SO_4\ (s) + Na_2SO_4\ (s) + NaLa(SO_4)_2\ (s) + 2SO_2\ (g) + O_2\ (g)$.

where $La_2(SO_4)_3$ is completely converted to $La_2O_2SO_4$ while $NaLa(SO_4)_2$ is partially converted to $La_2O_2SO_4$ and Na_2SO_4.

At 1000°C, only sulfur dioxide and oxygen have been removed, the sodium ions remain stable in the structures. In the structure of $La_2O_2SO_4$ [29] the lanthanum atom is coordinated by 8 oxygen by forming LaO_8 polyhedrons.

The three exothermal peaks on the DTA curve on cooling correspond to the crystallization of the three final phases $La_2O_2SO_4$, Na_2SO_4 and $NaLa(SO_4)_2$ characterized by x-ray powder diffraction.

III.3. Raman spectroscopy results:

The Raman spectra of the $NaLa(SO_4)_2.H_2O$, $Na_3La(SO_4)_3$ and $NaLa(SO_4)_2$ are shown in Figure 11. The zone-center irreducible representation of the phonon (accoustic and optical) modes in the hydrated compound is: $\Gamma[NaLa(SO_4)_2.H_2O] = 21\ A_1 \oplus 24\ A_2 \oplus 45\ E$, where the E-representation is both Raman and infrared active and the A_1 (resp A_2) representation is Raman (resp. infrared) active. For the anhydrous compounds, the irreductible representations become: $\Gamma[Na_3La(SO_4)_3] = 18\ A_g \oplus 18\ E_g^* \oplus 20\ A_u \oplus 20\ E_u^*$ and $\Gamma[NaLa(SO_4)_2] = 36\ (A_g \oplus A_u)$, where the *gerade* (g) and *ungerade* (u) representations are Raman and infrared active, respectively. In the case of $Na_3La(SO_4)_3$, motions of the lanthanum atoms are forbidden in Raman due to the C_{3i}-site symmetry of the La-atoms (but allowed in infrared).

The assignment of the Raman lines is carried out based on the vibrations of the sulfate groups. A free sulfate ion belongs to the T_d molecular point group and its irreducible representation for the internal modes is $A_1 \oplus E \oplus 2F_2$, where these three representations are Raman active whereas only the F_2 one is infrared active. These modes correspond in the Herzberg's notation

[30] to the nine intramolecular modes labelled: ν_1, ν_2, ν_3 and ν_4. The nondegenerate $\nu_1(A_1)$ (resp. triply degenerate $\nu_3(F_2)$) vibration is a symmetric (resp. antisymmetric) stretching located around 983 cm^{-1} (resp. 1105 cm^{-1}). The remaining modes are deformation modes. The symmetric deformation, $\nu_2(E)$, is doubly degenerate and located about 450 cm^{-1} whereas the asymmetric one, $\nu_4(F_2)$, is triply degenerate and centered about 611 cm^{-1}. The low site symmetry (C_1) of the sulfate groups in the three compounds lifts all the degeneracies of the T_d molecular point group to yield to a unique non-degenerate A-representation. The correlation procedure between the free SO_4 groups of T_d symmetry, C_1-site symmetry and the factor group symmetry in $NaLa(SO_4)_2.H_2O$, $Na_3La(SO_4)_3$ and $NaLa(SO_4)_2$ is listed in Table 2.

The strong lines within the 950-1030 cm^{-1} range observed in Figure 11 are assigned to $\nu_1(A_1)$ symmetric stretching vibrations whatever the compound. Only one line is observed in $NaLa(SO_4)_2.H_2O$ (1010 cm^{-1}) and $Na_3La(SO_4)_3$ (980 cm^{-1}) whereas two lines are observed (995 and 1012 cm^{-1}) in $NaLa(SO_4)_2$. This difference is a consequence that $NaLa(SO_4)_2$ is characterized by two crystallographically independent sulfate groups whereas the two other compounds has only one independent sulfate group. The lines above 1030 cm^{-1} are assigned to $\nu_3(F_2)$ vibrations in the three compounds. The $n_4(F_2)$ vibrations are evidenced within the 550-700 cm^{-1} range whereas the $n_2(E)$ vibrations are assigned in the 400-550 cm^{-1} range. The number of Raman lines expected by the group theory within the sulfate vibration regions is clearly seen in the case of the anhydrous $NaLa(SO_4)_2$ compound. However, in the two other compounds, this number is smaller than that expected and polarized measurements could help to assign the missing lines. Below 400 cm^{-1}, translational, rotational and librational motions of the sulfate groups as rigid units are expected as well as motions of the other polyhedra.

IV. Conclusion

In this paper, the thermal stability of sodium lanthanum double sulfate monohydrate is revisited by using complementary experiments. In opposite to the literature, the dehydration (220-260°C) is not only a releasing of the water molecule but also a complete chemical transformation leading to the formation of a new kind of anhydrous Sodium Lanthanum triple sulfate $Na_3La(SO_4)_3$ (*R*-3) with LaO_{12} icosahedrons and of a sulfate of lanthanum. The water molecules inside the crystallographic tunnels of the initial monohydrate sulfate act as a network stabilizer. The removing of these water molecules leads to a complete restructuring of the crystalline framework leading to $Na_3La(SO_4)_3$. At 774°C, the DTA peak observed without any weight loss is due to the formation of the anhydrous sodium lanthanum double sulfate $NaLa(SO_4)_2$ (*P*-1) and Na_2SO_4. All these transformations are compatible with the Raman signatures expected in these compounds.

The complete reaction of $NaLa(SO_4)_2$, H_2O up to 800°C is given by:

$$3\ NaLa(SO_4)_2,H_2O\ (s) \rightarrow\ NaLa(SO_4)_2\ (s) + Na_2SO_4\ (s) + La_2(SO_4)_3\ (s) + 3H_2O(g)$$

At 1000°C, the sulfate anions begin to be removed and a global chemical reaction is proposed as:

$$3\ NaLa(SO_4)_2,H_2O\ (s) \rightarrow La_2O_2SO_4\ (s) + Na_2SO_4\ (s) + NaLa(SO_4)_2\ (s) + 3H_2O(g) + 2SO_2\ (g) + O_2\ (g).$$

With these results, the mechanism of the thermal conversion of $NaLa(SO_4)_2,H_2O$ is now well established with the identification of the structure of a new triple sulphate of formula $Na_3La(SO_4)_3$ coming from the dehydration of the monohydrate. All $NaLn(SO_4)_2,H_2O$

compounds are isostructural to $NaLa(SO_4)_2,H_2O$ with the trigonal $P3_121$ space group. Therefore, the dehydration mechanism proposed for *Ln*= La could be ~~applied~~ verified to the other compounds with *Ln*= Ce, Pr, Nd….

The chemistry of lanthanide-based compounds is very rich because of the great variability of their structure. This is due to the presence of lanthanides that can adopt a highly variable coordinence number from 8 to 12. In consequence, if the dehydration mechanism is identical in the $NaLn(SO_4)_2,H_2O$ family, that could open the way to a new series of Lanthanides trisulfates with the general chemical formula $Na_3Ln(SO_4)_3$ with other optical properties.

References

[1] Ruiz-Valero, C. ; Cascales, C. ; Gomez-Lor, B. ; Gutierrez-Puebla, E. ; Iglesias, M. ; Monge, M.A. ; Snejko, N. J. New catalytically active neodymium sulfate. *J. of Mater. Chem.* 2002, 12, 3073.

[2] Perles, J. ; Fortes-Revilla, C. ; Gutierrez-Puebla, E. ; Iglesias, M. ; Monge, M.A. ; Ruiz-Valero, C. ; Snejko, N. Synthesis, structure and catalytic properties of rare-earth ternary sulfates, *Chem. Mater.* 2005, 17, 2701. DOI: 10.1021/cm049451z

[3] Ramya, A.R. ; Sharma, D. ; Natarajam S. ; Reddy, M.L.P. Highly Luminescent and Thermally Stable Lanthanide Coordination Polymers Designed from 4-(Dipyridin-2-yl)aminobenzoate: Efficient Energy Transfer from Tb^{3+} to Eu^{3+} in a Mixed Lanthanide Coordination Compound. *Inorg. Chem*., 2012, 51, 8818.

[4] Höppe, H.A. ; Recent Developments in the Field of Inorganic Phosphors. *Angew. Chem. Int. Ed*., 2009, 48, 3572.

[5] Mahata, P. ; Ramya, K.V. ; Natarajan, S. Pillaring of $CdCl_2$-Like Layers in Lanthanide Metal–Organic Frameworks: Synthesis, Structure, and Photophysical Properties. *Chem. A Eur. J*., 2008, 19, 5839.

[6] Shehee, T.C. ; Sykora, R.E. ; Ok, K.M. ; Halasyamani, P.S. ; Albert-Schmitt, T.E. Hydrothermal Preparation, Structures, and NLO Properties of the Rare Earth Molybdenyl Iodates, $RE(MoO_2)(IO_3)_4(OH)$ [RE = Nd, Sm, Eu]. *Inorg. Chem*.,2003, 42, 457.

[7] Jüstel, T. ; Nikol, H. ; Ronda, C. New Developments in the Field of Luminescent Materials for Lighting and Displays. *Angew. Chem. Int. Ed*., 1998, 37, 3084.

[8] Junk, P.C. ; Kepert, C.J. ; Skelton, B.W. ; White, A.H. Structural Systematics of Rare Earth Complexes. XX (Maximally) Hydrated Rare Earth Sulfates and the Double Sulfates $(NH_4)Ln(SO_4)_2.4H_2O$ (Ln = La, Tb). *Aus. J. Chem*., 1999, 52, 601.

[9] Wickleder, M.S. Synthese, Kristallstrukturen und Thermisches Verhalten von $Er_2(SO_4)_3.8H_2O$ und $Er_2(SO_4)_3.4H_2O$. *Z. Anorg. Allg. Chem*., 1999, 625, 1548.

[10] Wickleder, M.S. Inorganic Lanthanide Compounds with Complex Anions. *Chem. Rev*., 2002, 102, 2011.

[11] Robinson, P.D.; Jasty, S. A 2-Alkyl Substituted 2,3,1-Benzodiazaborine. *Acta Crystallogr*., 1998, C54, 1.

[12] Sarukhanyan, N.L. ; Iskhakova, L.D. ; Trunov, V.K. ; Ilyukhin, V.V. Crystal structure of $RbLn(SO_4)_2.xH_2O$ (Ln=Gd, Ho, Yb), *Koordinatsionnaya Khimiya*, 1984, 10(7), p. 981-987

[13] Blackburn, A.C. ; Gerkin, R.E. Redetermination of Sodium Cerium(III) Sulfate Monohydrate, $NaCe(SO_4)_2.H_2O$. *Acta Crystallogr*., 1995, C51, 2215.

[14] Iskhakova, L.D.; Bondar', S.A. ; Trunov, V.K. Crystallohydrate $LiCe(SO_4)_2 \cdot H_2O$ and some regularities of structure of $MTR(SO_4)_2 \cdot H_2O$ (M=Li-Rb), *Kristallografiya,* 1987, 32, 328.

[15] Blackburn, A.C. ; Gerkin, R.E. Sodium lanthanum(III) sulfate monohydrate, $NaLa(SO_4)_2.H_2O$. *Acta Crystallogr*., 1994, C50, 835.

[16] Jemmali, M. ; Walha, S. ; Ben Hassen, R. ; Vaclac, P. Potassium cerium(III) bis(sulfate) monohydrate, $KCe(SO_4)_2.H_2O$. *Acta Crystallogr C*, 2005, 61, i73-5. DOI: 10.1107/S0108270105006219

[17] Iskhakova, L.D.; Gasanov Y.M.; Trunov, V.K. Crystal structure of the monoclinic modification of $KNd(SO_4)_2$ *Journal of Structural Chemistry*, 1988, 29, 242–246.

[18] Buyer, C.; Enseling, D.; Jüstel, T.; Schleid, T. Hydrothermal Synthesis, Crystal Structure, and Spectroscopic Properties of Pure and Eu^{3+}-Doped $NaY[SO_4]_2.H_2O$ and Its Anhydrate $NaY[SO_4]_2$. *Crystals*, 2021, 11, 575. DOI: 10.3390/cryst11060575.

[19] Sarukhanyan, N.L.; Iskhakova, L.D. ; Drobinskaya, I.G. ; Trunov, V.K. Crystal structure of $KLu(SO_4)_2.2H_2O$. *Kristallografiya*, 1985, 30, 880-884.

[20] Porvali, A. ; Wilson, B.P. ; Lundström, M. Lanthanide-alkali double sulfate precipitation from strong sulfuric acid NiMH battery waste leachate. *Waste Management*, 2018, 71, 381.

[21] Lindgren, O. the crystal structure of sodium cerium (III) sulfate hydrate $NaCe(SO_4)_2.H_2O$. *Acta Chem. Scand.* 1977, A31, 591.

[22] Paul, A.K. ; Kanagaraj, R. Synthesis, characterization, and crystal structure analysis of new mixed metal sulfate $NaPr(SO_4)_2.H_2O$. *J. of Struct. Chem.* 2019, 3, 477.

[23] Kazmierczak, K. ; Höppe, H.A. Syntheses, crystal structures and vibrational spectra of $KLn(SO_4)_2.H_2O$ (Ln=La, Nd, Sm, Eu, Gd, Dy) *J. Solid State Chem.,* 2010, 109, 2652.

[24] Kolcu, Ö. ; Zümreoglu-Karan, B. Thermal properties of sodium-light-lanthanoid double sulfate monohydrates *Thermochimica Acta,* 1994, 240, 185.

[25] Denisenko Y.G.; Sedykh A.E.; Basova S.A.; Atuchin V.V.; Molokeev M.S. Aleksandrovsky A.S.; Krylov A.S.; Oreshonkov A.S.; Khritokhin N.A.; Sal'nikova E.I.; Andreev O.V.; Müller-Buschbaum K. Exploration of the structural, spectroscopic and thermal properties of double sulfate monohydrate $NaSm(SO_4)_2.H_2O$ and its thermal decomposition product $NaSm(SO_4)_2$. *Advanced Powder Technology*, 2021, Volume 32, Issue 11**,** Pages 3943-3953. DOI: 10.1016/j.apt.2021.08.009.

[26] Buyer C.; Enseling D.; Jüstel T.; Shield T. Hydrothermal synthesis, crystal structure and spectroscopic properties of pure and Eu^{3+}-doped $NaY(SO_4)_2.H_2O$ and its anhydrate $NaY(SO_4)_2$. *Crystals* 2021, 11, 575. DOI: 10.3390/cryst11060575.

[27] Chizhov, S.M.; Pokrovskii, A.N.; Kovba, L.M. The crystal structure of $NaLa(SO_4)_2$. *Kristallografiya*, 1981, 26, 834-836.

[28] Poston J.A.; Siriwardane R.V.; Fisher E.P.; Miltz A.L. thermal decomposition of the rare earth sulfates of ceriem(III), cerium(IV), lanthanum(III) and samarium(III). *Applied Surface Science*, 2003, 214, 83–102. DOI:10.1016/S0169-4332(03)00358-1.

[29] Zhukov, S.G.; Yatsenko, A.; Chernyshev, V.V.; Trunov, V.; Tserkovnaya, E.; Antson, O.; Hoelsae, J.; Baules, P.; Schenk, H. Structural study of lanthanum oxysulfate $(LaO)_2SO_4$. *Materials Research Bulletin*, 1997, 32, 43-50. DOI: 10.1016/S0025-5408(96)00159-6.

[30] G. Herzberg. Infrared and Raman Spectra of Polyatomic Molecules. Ed. Van Nostrand (1945).

[31] K. Momma and F. Izumi, VESTA 3 for three-dimensional visualization of crystal, volumetric and morphology data*, J. Appl. Cryst*. (2011). 44, 1272-1276.

FIGURES

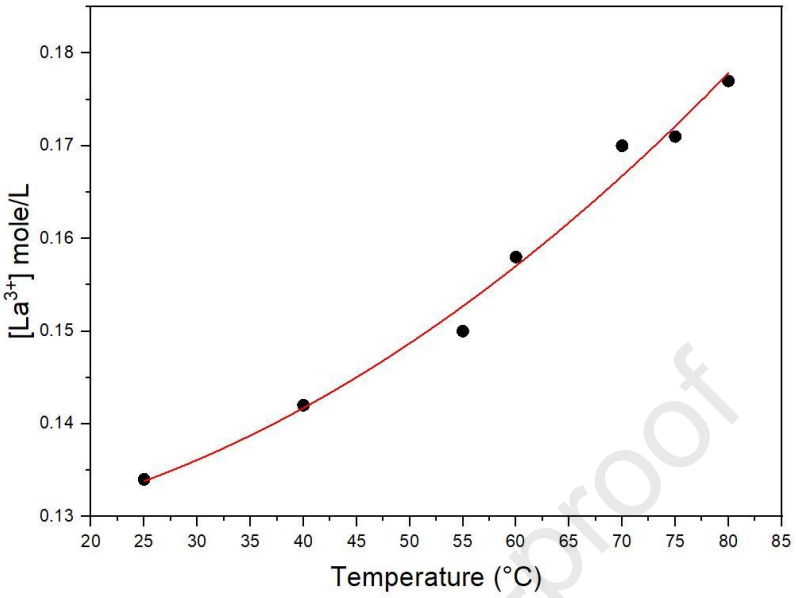

Figure 1: Solubility curve of $NaLa(SO_4)_2,H_2O$ in 4M HCl.

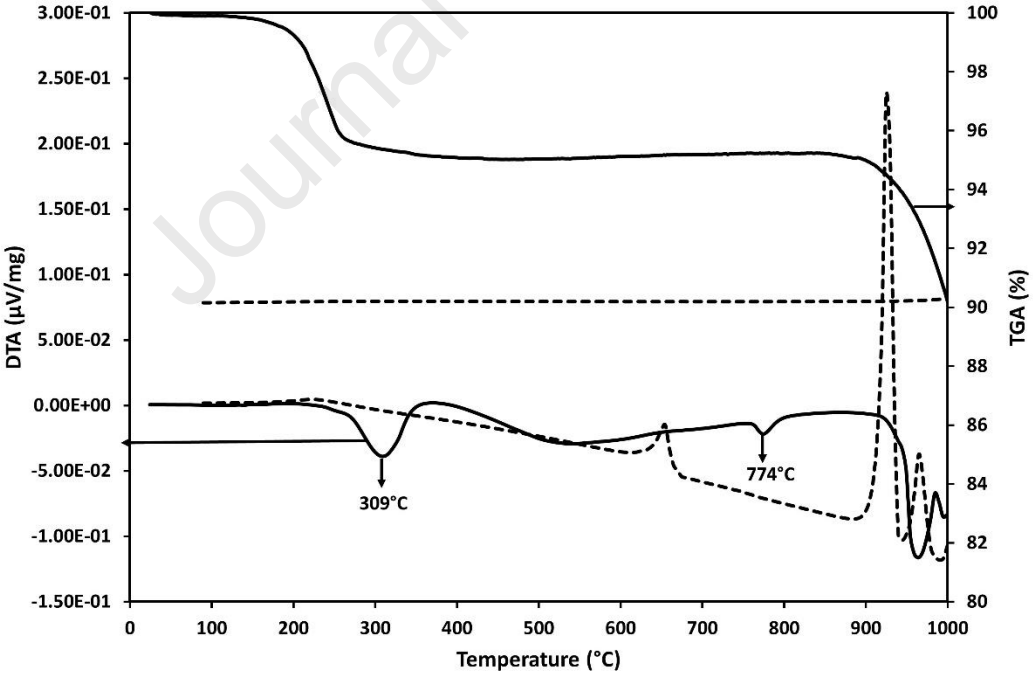

Figure 2: TGA-DTA analyze of $NaLa(SO_4)_2,H_2O$ (heating: full line; cooling: dotted line)

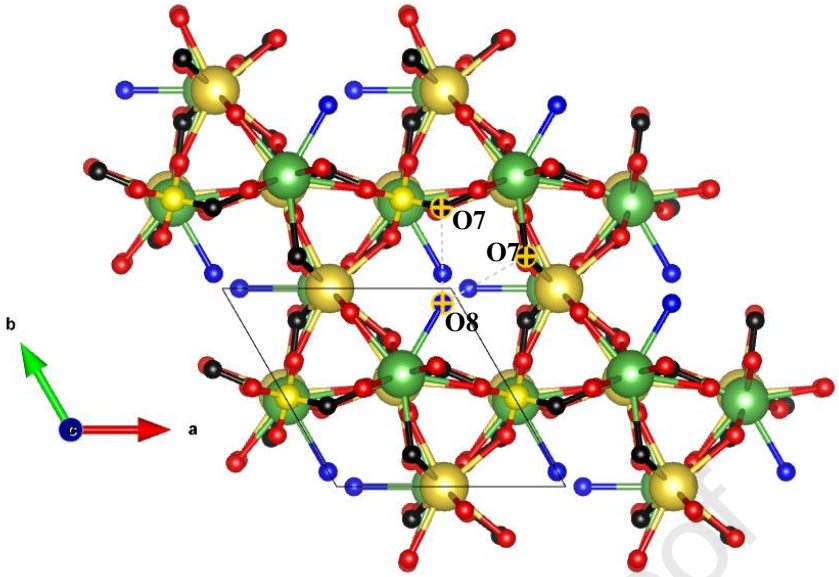

Figure 3: Structure of $NaLa(SO_4)_2$, H_2O viewed along the <001> direction [31]. O atom in blue and "O8" labelled is that of water molecule. O7 (in black) are the oxygen atoms connected to the O8 atom via an H-bond

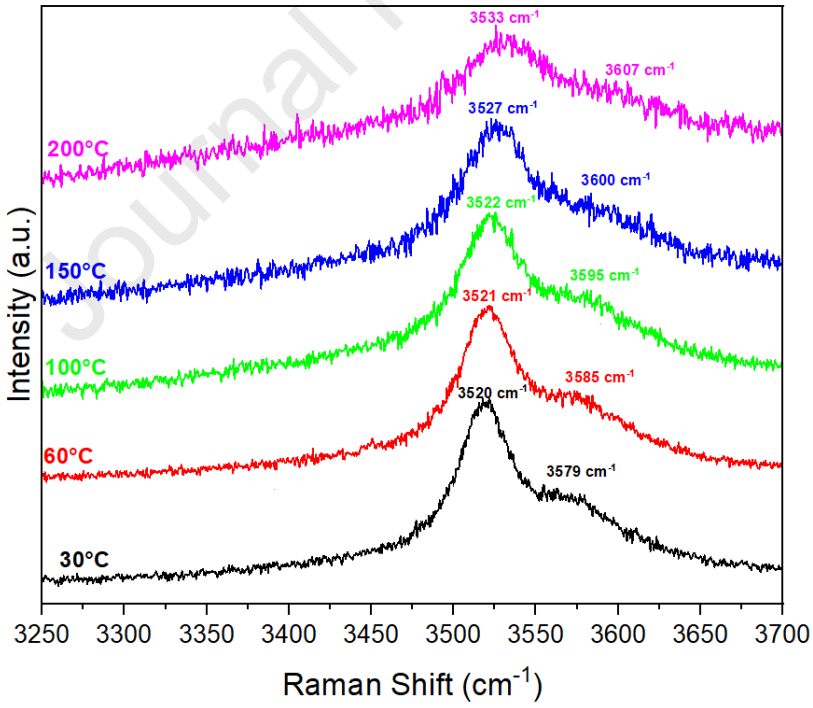

Figure 4: Raman spectra of the OH stretching vibrations (3250 – 3700 cm^{-1}) between 30 and 200°C.

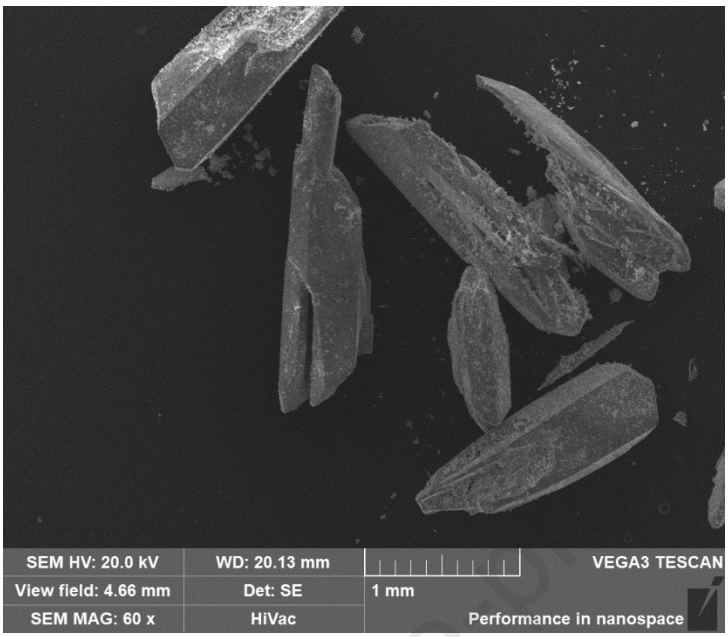

Figure 5: $Na_3La(SO_4)_3$ single crystals grown under hydrothermal conditions (300°C, 157bars)

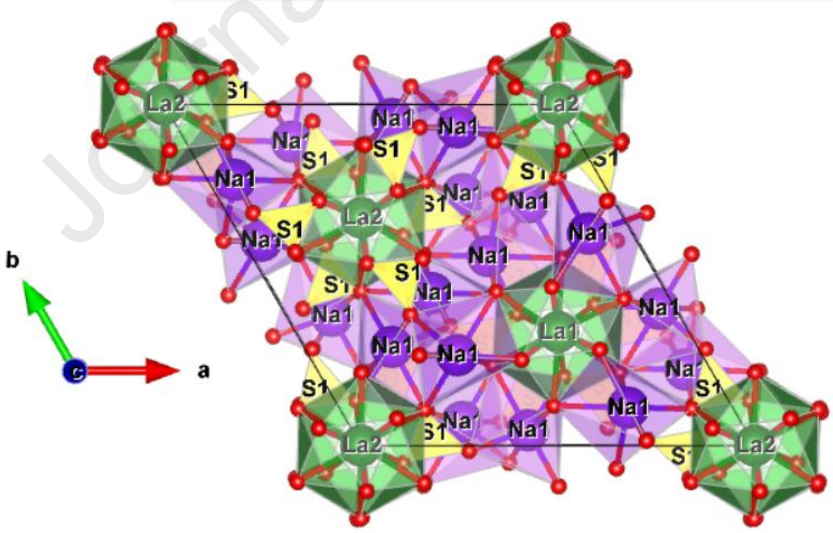

Figure 6: Structure of $Na_3La(SO_4)_3$ viewed along the <001> direction [31]

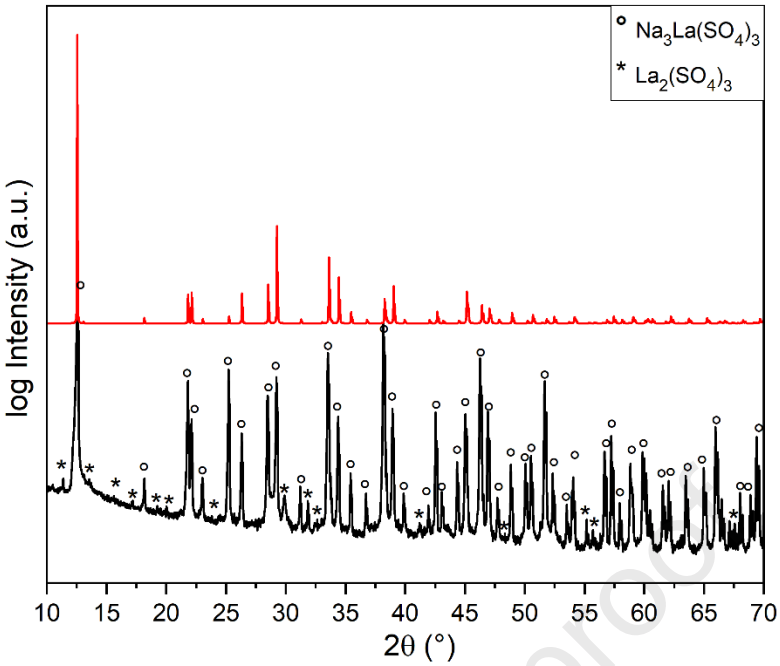

Figure 7: X-ray powder diffraction pattern of the powder (bottom) obtained after a thermal treatment at 300°C. Calculated pattern of $Na_3La(SO_4)_3$ (*R*-3) issued from the single crystal x-ray diffraction is given in reference (up).

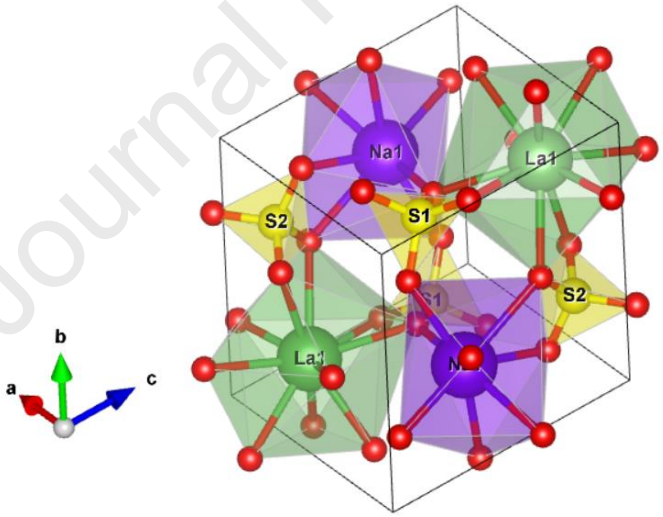

Figure 8: Structure of $NaLa(SO_4)_2$ [31]

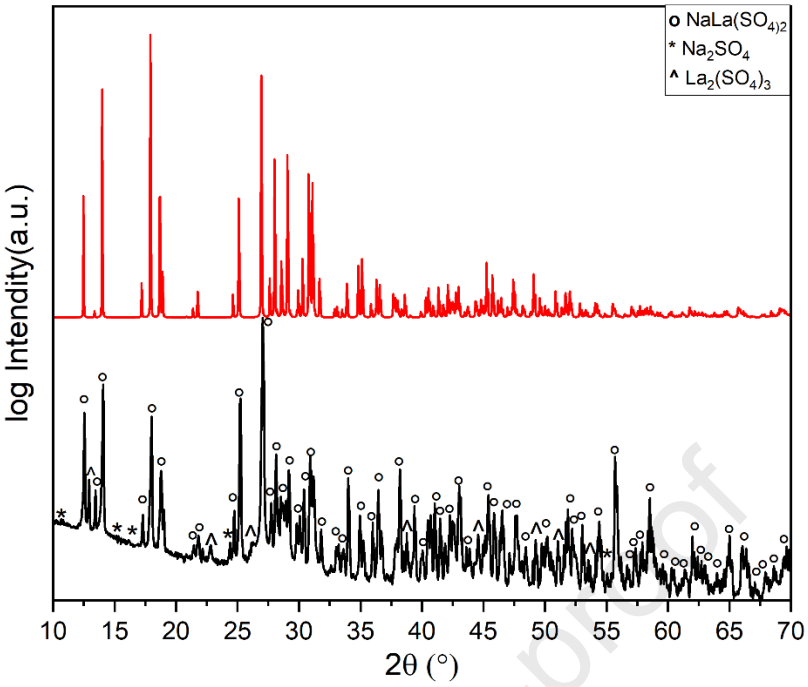

Figure 9: X-ray powder diffraction pattern of the powder (bottom) after a thermal treatment at 800°C. Calculated pattern of $NaLa(SO_4)_2$ (*P*-1) from the single crystal x-ray diffraction is given in reference (up).

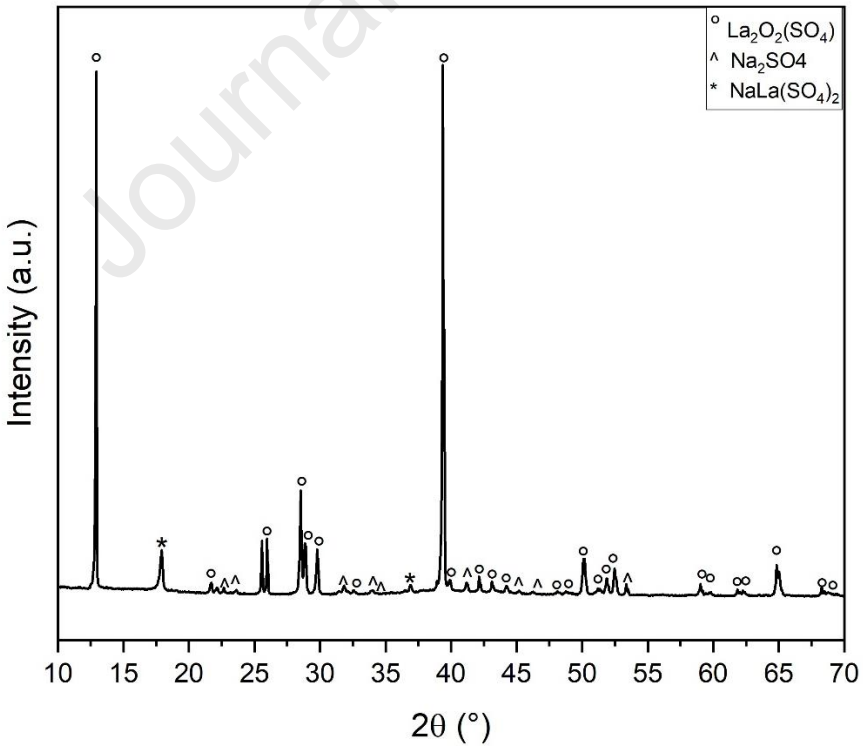

Figure 10: X-ray powder diffraction pattern of the compounds after a thermal treatment at 1000°C.

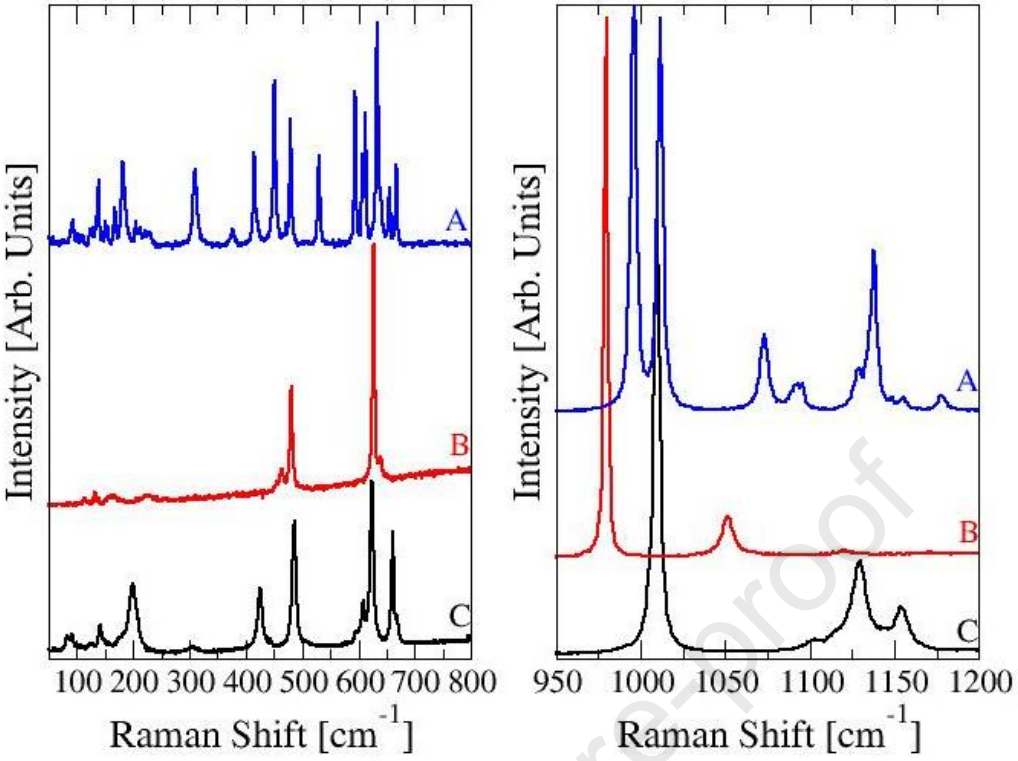

Figure 11: Room temperature Raman spectra of
A- $NaLa(SO_4)_2$ *P*-1 (T_c= 800°C).
B- $Na_3La(SO_4)_3$ *R*-3 (T_c= 300°C).
C- $NaLa(SO_4)_2,H_2O$ $P3_121$ (T_c=80°C).

TABLES

Table 1: Data collection, Refinement and Crystal data

	$NaLa(SO_4)_2,H_2O$	$Na_3La(SO_4)_3$	$NaLa(SO_4)_2$
Synthesis Temperature (°C)	80	300	800
CCDC deposition number	2174475	2168542	2169024
XRD Temperature (K)	294	100	293
molar weight ($g.mol^{-1}$)	370.02	496.06	354.02
Space group	$P3_121$	R-3	P-1
a (Å)	7.0516(1)	14.0976(1)	7.100(3)
b (Å)	7.0516(1)	14.0976(1)	6.779(3)
c (Å)	12.9587(2)	8.1267(1)	6.473(3)
α (°)	90	90	77.701(14)
β (°)	90	90	91.313(14)
γ (°)	120	120	92.705(14)
Z	3	6	2
calc. density ($g.cm^{-3}$)	3.303	3.533	3.867
μ (mm^{-1})	7.943	43.87	7.79
dimension (mm)	0.202x0.201x0.150	0.15x0.08x0.02	0.12x0.08x0.02
Wavelenght (Å)	0.71073	1.54184	0.71073
Diffractometer	BRUKER D8 Venture Photon II detector	RIGAKU XtaLAB Synergy	BRUKER Kappa Apex2
h, k, l range	(-15,-15,-28) to (15,15,28)	(-17,-17,-9) to (17,17,6)	(-12,-11,-11) to (12,11,11)
θ range (°)	3.336 to 52.308	6.3 to 79.7	2.9 to 38.1
Reflections measured	28806	13928	16175
Independent reflections	4241	593	3208
Reflexions with $I>2\sigma(I)$	4241	591	3208
$R[I>2\sigma(I)]$	0.0146	0.016	0.019
$wR(F^2)$	0.036	0.042	0.048
Absorp. Correction	Multi-scan SADABS method	multiscan Crysalis Pro. Spherical harmonics (Scale3 Abspack)	Multi-scan SADABS (Siemens 1996)

Table 2: Correlation scheme between the T_d molecular point group, C_1-site symmetry and the factor group symmetry for one independent sulphate group in $NaLa(SO_4)_2.H_2O$ (D_3^4), $Na_3La(SO_4)_3$ (C_{3i}^2) and $NaLa(SO_4)_2$ (C_i^1).

T_d point group	**C_1 Site symmetry**	**$S_6=C_{3i}$ Factor group symmetry**	**C_i Factor group symmetry**	**D_3 Factor group symmetry**
A_1 (ν_1)	A	$A_g \oplus 2E_g^* \oplus A_u \oplus 2E_u^*$	$A_g \oplus A_u$	$A_1 \oplus A_2 \oplus 2E$
E (ν_2)	2A	$2(A_g \oplus 2E_g^* \oplus A_u \oplus 2E_u^*)$	$2(A_g \oplus A_u)$	$2(A_1 \oplus A_2 \oplus 2E)$
F_2 (ν_3)	3A	$3(A_g \oplus 2E_g^* \oplus A_u \oplus 2E_u^*)$	$3(A_g \oplus A_u)$	$3(A_1 \oplus A_2 \oplus 2E)$
F_2 (ν_4)	3A	$3(A_g \oplus 2E_g^* \oplus A_u \oplus 2E_u^*)$	$3(A_g \oplus A_u)$	$3(A_1 \oplus A_2 \oplus 2E)$

TOC

Highlights

The structural stability of $NaLa(SO_4)_2,H_2O$ ($P3_121$) up to 200°C is ensured by the water molecules located in channels along the c-axis. The dehydration after 260°C leads to a drastic modification of the crystalline network. At 300°C, a new triple sulphate $Na_3La(SO_4)_3$ crystallizes in the *R*-3 space group with LaO_{12} icosahedrons. At 800°C, $Na_3La(SO_4)_3$ decomposes by forming the anhydrous double sulfate $NaLa(SO_4)_2$ crystallizing in the *P*-1 space group with LaO_{10} polyhedra.

Graphic

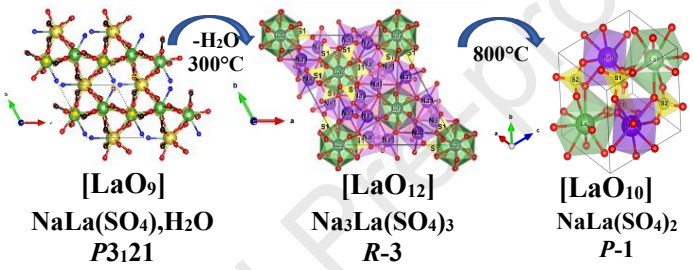

Highlights

- The structural stability of $NaLa(SO_4)_2,H_2O$ with LaO_9 polyhedrons up to 200°C is ensured by the water molecules located in channels along the *c*-axis.
- At 260°C, the dehydration of $NaLa(SO_4)_2,H_2O$ leads to the formation of a new triple sulphate $Na_3La(SO_4)_3$ crystallizing in the *R*-3 space group with LaO_{12} icosahedrons.
- $Na_3La(SO_4)_3$ crystal growth under (300°C-157bars) hydrothermal conditions.
- After 774°C, $Na_3La(SO_4)_3$ decomposes by forming the anhydrous double sulfate $NaLa(SO_4)_2$ crystallizing in the *P*-1 space group with LaO_{10} polyhedra.

Declaration of interests

☒ The authors declare that they have no known competing financial interests or personal relationships that could have appeared to influence the work reported in this paper.

☐ The authors declare the following financial interests/personal relationships which may be considered as potential competing interests: